Tropical Cyclone Central Pressure Estimation Using Doppler Radar Observations at JMA

Udai Shimada

Meteorological Research Institute, Japan Meteorological Agency

Abstract

The Meteorological Research Institute of the Japan Meteorological Agency has developed a new system for estimating the intensity (central pressure) of tropical cyclones (TCs) at 5-min intervals using single ground-based Doppler radar observations. The method involves the use of the ground-based velocity track display (GBVTD) technique, in which tangential winds are retrieved, and the gradient wind balance. In terms of the accuracy of this method, the root mean square error (RMSE) and bias are 8.37 and 1.51 hPa, respectively, to the best track data of the Regional Specialized Meteorological Center (RSMC) Tokyo. This level of accuracy is comparable to or better than the accuracies of conventional methods such as Dvorak and satellite microwave-derived estimates. In particular, for TCs with a radius of maximum wind of 20 – 70 km, the estimated central pressures have an RMSE of 5.55 hPa. The method enables TC monitoring at 5-min intervals from several hours before landfall in populated areas and helps to clarify intensity changes in real time. This report details the characteristics, utilities and limitations of the Doppler radar intensity estimation method and outlines examples of related estimation.

1. Introduction

Highly accurate analysis of tropical cyclone (TC) intensity (i.e., central pressure and maximum sustained wind) is important for real-time TC monitoring and TC intensity forecasting. The Regional Specialized Meteorological Center (RSMC) Tokyo analyzes TC intensity on the basis of Dvorak estimates (Dvorak 1975, 1984; Koba et al. 1990; Kishimoto et al. 2013) with appropriate adjustments using Advanced Microwave Sounding Unit (AMSU) estimates (AMSU method, Oyama 2014), satellite microwave imager estimates (Hoshino and Nakazawa 2007; Sakuragi et al. 2014) and all other available observations. The Dvorak technique supports the provision of estimates at 6-hr intervals in real time, but involves a relatively large margin of error with a standard deviation of 7 – 19 hPa (Koba et al. 1990). The AMSU method does not provide TC intensity estimation in real time due to data latency and also has a weakness

associated with poor data resolution. There is a strong need for estimation of TC intensity with as much accuracy as possible, particularly for TCs that approach populated areas. As the conventional methods described above involve statistical estimation of TC intensity based on relevant physical values such as cloud patterns and upper-level warm core anomalies, there are inevitably limitations to their accuracy. For more accurate estimation, a method involving the use of a straightforward physical equation that describes pressure distribution is required.

Lee et al. (1999, 2000) developed a method involving the use of data from a single ground-based Doppler radar (DR) (hereafter, the DR method). This approach leverages the ground-based velocity track display (GBVTD) technique (Lee et al. 1999), in which axisymmetric tangential wind velocities ($\bar{V}_t$) are retrieved from Doppler radial velocities (V_D), and the gradient wind balance equation, from which an axisymmetric pressure deficit is deduced for estimation of minimum sea level pressure (MSLP). As the DR method involves the use of a straightforward physical equation, if sufficient V_D coverage is available and a TC has circular wind fields above the boundary layer that approximately satisfy the gradient wind equation, MSLPs can generally be provided with high accuracy. In addition, the approach involves real-time estimation of MSLP at 5-min intervals, which enables monitoring of rapid TC intensity changes. Although the DR method can be applied only when a TC is within areas of radar observation, it enables estimation of intensity from several hours before landfall in populated areas and the avoidance of situations in which TC analysts can gauge exact intensity only upon landfall. Thus, the DR method is promising if estimate accuracy is ensured.

The Meteorological Research Institute of the Japan Meteorological Agency (MRI/JMA) developed a system for estimating TC intensity using the DR method. The approach is similar to that of the Vortex Objective Radar Tracking and Circulation (VORTRAC) system (Harasti et al. 2007) already implemented by the National Hurricane Center (NHC). Shimada et al. (2016, hereafter SSY) applied the DR method to estimate intensities of TCs approaching Japan between 2006 and 2014, and investigated the accuracies and utilities of the method. SSY showed that most DR estimates were plausible despite some significant differences from the best-track data of RSMC Tokyo. This report presents a number of important points regarding the DR method from the perspective of operational use. In particular, the characteristics of DR estimates relative to the best-track data are described, and the DR method's applicability to real-time estimation of plausible MSLPs is emphasized. Readers interested in the technical details are referred to SSY.

This report consists of five sections. Section 2 describes the method and its limitations,

Section 3 highlights the accuracy and validity of the DR method, Section 4 presents several characteristics of DR estimates and related examples, and Section 5 summarizes the report.

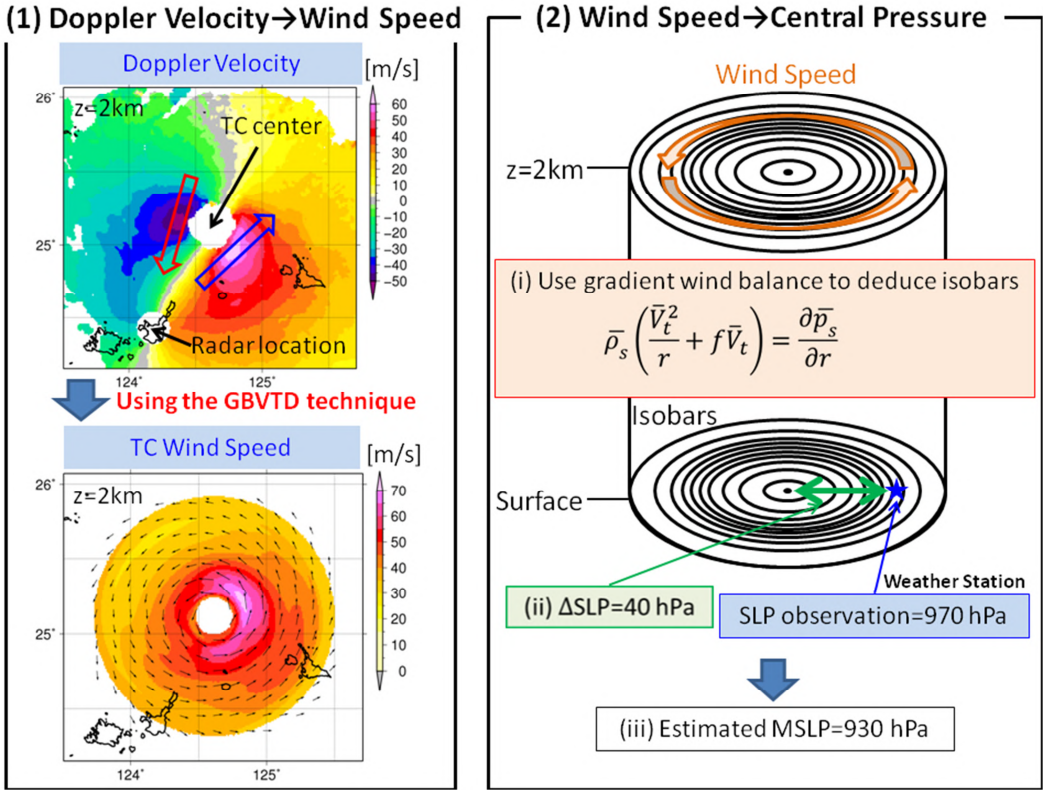

Fig. 1: DR method procedures

2. Method and limitations

2.1 Method

Figure 1 shows schematics of the DR method, which has two main steps. The first involves the retrieval of $\bar{V}_t$ at 2-km altitude from V_D using the GBVTD technique, whose limitations are described in the next subsection. The second step involves the deduction of axisymmetric pressure deficit distribution at sea level based on application of the retrieved $\bar{V}_t$ to the gradient wind equation

$$\bar{\rho_s}\left(\frac{\bar{V}_t^2}{r}+f\bar{V}_t\right)=\frac{\partial\bar{p_s}}{\partial r} \qquad (1),$$

where r is the radius from the TC center, f is the Coriolis parameter corresponding to the latitude of each radar location, $\bar{p_s}$ is axisymmetric sea level pressure (SLP) and $\bar{\rho_s}$ is environmental air density at sea level. MSLP is then estimated based on the pressure deficit distribution and SLP observation around the TC as an anchor for pressure

measurement. The number of MSLPs estimated corresponds to the number of SLP observations, and estimation is performed at 5-min intervals.

The DR method includes the assumption that $\bar{V}_t$ at 2-km altitude is within the gradient wind balance. This is rational because previous studies based on observations and numerical simulations have shown the validity of the gradient wind balance approximation above the boundary layer (e.g., Bell and Montgomery 2008; Willoughby 1990; Ogura 1964; Kepert 2006a, b). It should be noted that the gradient wind balance is satisfied in terms of azimuthally averaged wind and pressure gradient, but not satisfied locally (Willoughby 1990).

2.2 Limitations

This subsection describes the limitations of the DR method in three parts: limitations inherent in the GBVTD technique, limitations relating to radar data quality, and other limitations. It is important that analysts adopting the DR method for TC intensity analysis fully recognize these limitations, as they directly affect the quality of estimates. See Table 1 for a summary.

a. Limitations inherent in the GBVTD technique

The GBVTD technique can be applied to retrieve tangential winds (up to wavenumber 3) and radial winds (only wavenumber 0) of a TC and the component of the mean environmental wind parallel to a line connecting the TC center and the radar location at each radius of the TC. This is based on the assumption that there is one primary circular vortex around the TC center and that the extent of asymmetric radial wind is much smaller than that of the corresponding tangential wind (Lee et al. 1999). For TCs with wind fields that violate this assumption, GBVTD retrieval errors are inevitably large, leading to significant errors in estimated MSLPs. Five limitations of the GBVTD technique should be noted in relation to application of the DR method.

The first is the sensitivity of the GBVTD technique to errors of TC center detection (limitation I). In the DR method, the TC center is defined as the location at which the GBVTD-retrieved $\bar{V}_t$ is maximized for the radius of maximum wind (RMW) (Lee and Marks 2000). Lee and Marks (2000) showed that values of GBVTD-retrieved $\bar{V}_t$ can fluctuate significantly even with only minor deviations from the true center, and Harasti et al. (2004) showed that sensitivity to center locations can cause erratic fluctuations in estimated MSLPs.

The second limitation relates to the fact that the GBVTD technique cannot be used to retrieve the cross-beam (the normal to the line connecting the radar with the TC center)

component of mean environmental wind, $V_{M\perp}$ (limitation II). Instead, $V_{M\perp}$ is aliased into $\bar{V}_t$, which reduces the retrieval accuracy of $\bar{V}_t$ at outer TC radii (Lee et al. 1999; Harasti et al. 2004; Chen et al. 2013). To resolve this aliasing problem, $V_{M\perp}$ must be obtained from an independent source. The DR method outlined here involves the use of the cross-beam component of TC translational speed as a proxy for $V_{M\perp}$. SSY showed the effect of using this proxy on the accuracy of estimated MSLPs and demonstrated that large positive biases decreased to some extent as a result of its application.

The third limitation involves an issue relating to the aliasing of wavenumber-2 radial winds into $\bar{V}_t$ (see Lee et al. 1999; Murillo et al. 2011, limitation III). The GBVTD technique involves the assumption that asymmetric radial wind is much smaller than the corresponding tangential wind. However, if wavenumber-2 radial winds are dominant within the eye region and their distribution moves around the eyewall cyclonically together with mesovortices (e.g., Kossin and Schubert 2004; Braun et al. 2006) or vortex Rossby waves (e.g., Montgomery and Kallenbach 1997; Wang 2002), they can cause a bias in the retrieved $\bar{V}_t$ with a period of a few hours. As a result, this aliasing is likely to cause wavy fluctuations in estimated MSLPs with a period of a couple of hours.

The fourth limitation involves the emergence of a false local maximum of the GBVTD-retrieved $\bar{V}_t$ inside the actual RMW when strong mesovortices are likely to be present (e.g., Aberson et al. 2006; Marks et al. 2008) inside the eyewall (limitation IV). This can cause negative biases of estimated MSLPs. Some quality control (QC) processes can eliminate such false $\bar{V}_t$ maxima, but sometimes remove more of the GBVTD-retrieved $\bar{V}_t$ than necessary, leading to positive biases.

The fifth limitation involves the fact that wavenumber-1 tangential winds can cause biases in $\bar{V}_t$ via the nonlinear azimuthal coordinate system employed in the technique, particularly when the radar is around the radius of the GBVTD analysis ring (limitation V; see Fig. 13 (a) of Lee et al. 1999). This can lead to poor MSLP estimations, especially when the distance between the TC center and the weather station whose sea level pressure is used as the anchor for pressure measurement is close to that between the TC center and the radar location.

The sixth limitation involves the fact that the GBVTD technique cannot be used to retrieve $\bar{V}_t$ outside the radial distance from the TC center to the radar location (limitation VI). For example, if the radar is located inside the RMW associated with the primary eyewall, the GBVTD technique cannot be applied to retrieve $\bar{V}_t$ or estimate MSLPs due to a lack of V_D in the eye region.

Table 1: Summary of DR method limitations

	Limitation	Quality of retrieved $\bar{V}_t$	Effects on estimated MSLPs
I	TC center detection error	Erratic fluctuations	Erratic fluctuations
II	Aliasing of $V_{M\perp}$ into $\bar{V}_t$	Bias	Bias (both negative and positive)
III	Aliasing of wavenumber-2 radial winds into $\bar{V}_t$	Bias with a period of a few hours	Wavy fluctuations with a period of a couple of hours
IV	Effect of mesovortices inside eyewall	False maximum of $\bar{V}_t$ inside actual RMW	Negative bias
V	Bias effect of wavenumber 1 tangential wind on $\bar{V}_t$	Bias	Bias (both negative and positive)
VI	Limitation of retrieval area	Lack of retrieved $\bar{V}_t$	Absence of estimates
VII	Use of CAPPI data	Negative bias (weaker $\bar{V}_t$)	Positive bias
VIII	Noise contamination	Large errors	Large errors
IX	Lack of radar coverage	Bias	Large errors
X	Assumption of axisymmetricity	−	Errors
XI	Interpolation of missing $\bar{V}_t$	−	Errors
XII	Constant value of $\bar{\rho}_s$	−	Errors

b. Limitations relating to radar data quality

There are three limitations relating to radar data quality. The first is associated with constant-altitude plan position indicator (CAPPI) data at 2-km altitude with a radar range of around 200 km used in the DR method (limitation VII). Such data are compiled by interpolating plane position indicator (PPI) data with elevation angles of less than 10.0°. For radar ranges greater than around 130 km, V_D from the lowest-elevation PPI scan with a height between 2 and 4 km is projected onto the 2 km CAPPI. As vertical profiles of wind speed for TCs show a general increase from 3 km down to below 1 km (e.g., Franklin et al. 2003), this CAPPI method may contribute to positive MSLP biases if the TC center is far from the radar.

The second limitation involves noise contamination in radar data (limitation VIII). The maximum (Nyquist) velocity measurable by JMA C-band operational Doppler radars is around 52 m s^{-1}. Wind velocities greater than this are aliased. In addition, lower PPI contains sea clutter. Even when aliased V_D values are corrected by the method of Yamauchi et al. (2006) and sea clutter is removed, noise may remain and greatly affect the accuracy of the GBVTD-retrieved $\bar{V}_t$, leading to errors in TC intensity estimates.

The third limitation involves radar coverage (limitation IX), and is particularly

apparent with a disappearing eyewall. If coverage is sufficient for wind retrieval around the disappearing eyewall, estimated MSLPs will be toward the bottom of the range but still plausible. However, poor radar coverage around the disappearing eyewall will result in extremely high MSLPs (i.e., positively biased estimates). As a result, estimated MSLPs will fluctuate wildly between the two extremes.

c. Other limitations

The DR method has three other limitations. The first is the assumption that asymmetric components of pressure distribution are negligible (limitation X), which stems from the use of the gradient wind balance. This assumption can particularly affect the accuracy of estimates when SLP data observed far from the TC center are used in the second step of Fig. 1.

The second limitation involves the interpolation of $\bar{V}_t$ in the eye region where there are few scatterers (limitation XI). Under the DR method, missing $\bar{V}_t$ values are filled in using a spline function with the assumption that $\bar{V}_t$ = 0 m s^{-1} at the TC center. The radial distribution of $\bar{V}_t$ within the eye region is deduced in such a way, but this interpolation can result in estimation errors.

The third limitation involves the value of $\overline{\rho_s}$ used in Equation (1) (limitation XII). As the true value of $\overline{\rho_s}$ cannot be obtained, a value of 1.15 kg m^{-3} corresponding to density in a tropical environment with a virtual temperature of 30.0 °C at 1000 hPa is used in the DR method. At the second decimal place, this value may be a little higher than that in the TC inner environment, which would make the radial SLP gradient calculated from the gradient wind balance with Equation (1) slightly steeper than the actual gradient.

Table 2: Estimation accuracy for the six TCs obtained in the simulation experiment (data from SSY). Central pressure values were averaged over the estimation periods. For details, see SSY.

Case	Estimation period (UTC)	RMSE (hPa)	Bias (hPa)	Correlation	Central pressure (hPa)	
					Estimated	Actual
Overall	-	2.84	–0.77	0.95	-	-
S1215A	0200 26 Aug – 1500 26 Aug 2012	1.65	–0.25	-	933.61	933.86
S1215B	0200 26 Aug – 1500 26 Aug 2012	2.13	–0.82	-	932.55	933.37
S1408A	1900 07 Jul – 0110 08 Jul 2014	3.06	–1.50	-	929.46	930.97
S1408B	0100 08 Jul – 0410 08 Jul 2014	4.24	–3.55	-	924.96	928.51
S1408C	0100 08 Jul – 0700 08 Jul 2014	2.95	–1.96	-	926.22	928.18
S1419	0300 11 Oct – 1200 11 Oct 2014	4.47	3.28	-	950.10	946.81

3. Accuracy

This section describes the extent to which the DR method can be used to estimate MSLPs. The validity of the approach is first discussed, and its accuracy is then presented.

3.1 Validity of the DR method

To assess the validity of the DR method described in Subsection 2.1, SSY performed a preliminary experiment in which intensity was estimated using pseudo-V_D obtained from numerical simulation. This experiment helped to clarify the exact accuracy of the method because the actual value of central pressure is known from the simulation. In total, six cases involving three simulated TCs in the experiment were prepared, and intensity was estimated for each (see SSY for details). Table 2 shows the estimates in the preliminary experiment compared with the actual values for the simulated TCs. The RMSE of the estimated MSLPs relative to the actual MSLPs was 2.84 hPa, and the bias was –0.77 hPa despite relatively large errors in some cases. Thus, the experiment confirmed that the DR method can provide reasonable estimates of TC central pressure.

3.2 Estimation accuracy

This subsection details SSY's investigation of the DR method's accuracy, in which TC intensity was estimated using actual TCs and RSMC Tokyo best-track data as truth.

a. Overall accuracy

SSY estimated intensities for 28 cases involving 22 TCs that approached Japan between 2006 and 2014 (Table 3). If the same TC was observed by two or more radars, the observations of each radar were treated as a single case and the cases were distinguished by appending the letters A, B, or C to the TC name. The estimated duration of each was about 9 h on average.

The root mean square error (RMSE) and bias of the DR method were 8.37 and 1.51 hPa, respectively. A scatter diagram of the estimated and best-track MSLPs in the 28 cases shows that, despite large errors in some estimated MSLPs, most data points are concentrated in the vicinity of the 1:1 line (Fig. 2). The MSLP estimation error was within ±5 hPa (±10 hPa) in 60.3% (84.1%) of all estimates. Section 4 shows some examples where large errors were seen.

Table 4 shows the accuracy of the Dvorak and AMSU methods. The RMSE ranges from 7 to 19 hPa. These error statistics indicate that the accuracy of MSLP values obtained using the DR method is comparable to or better than those of the Dvorak and AMSU methods.

Table 3: Typhoons for intensity estimation (adapted from SSY)

Typhoon	Radar site	Estimation period (UTC)	Duration
T0607 (Maria)	Tokyo	0000 09 Aug – 0300 09 Aug 2006	3 h
T0709 (Fitow)	Tokyo	1600 06 Sep – 2300 06 Sep 2007	7 h
T0813 (Sinlaku)	Tanegashima	0200 18 Sep – 1500 18 Sep 2008	13 h
T0911 (Krovanh)	Tokyo	0600 31 Aug – 1000 31 Aug 2009	4 h
T1007 (Kompasu)	Okinawa	0200 31 Aug – 1300 31 Aug 2010	11 h
T1011 (Fanapi)	Ishigakijima	0500 18 Sep – 1900 18 Sep 2010	14 h
T1109 (Muifa)	Okinawa	1800 04 Aug – 1200 05 Aug 2011	18 h
T1115 (Roke)	Murotomisaki	2300 20 Sep – 0100 21 Sep 2011	2 h
T1204 (Guchol)	Okinawa	1000 18 Jun – 1500 18 Jun 2012	5 h
T1210 (Damrey)	Tanegashima	0100 01 Aug – 0900 01 Aug 2012	8 h
T1215 (Bolaven)	Okinawa	0400 26 Aug – 1700 26 Aug 2012	13 h
T1216 (Sanba)	Okinawa	1300 15 Sep – 0300 16 Sep 2012	14 h
T1217 (Jelawat)	Okinawa	1950 28 Sep – 0645 29 Sep 2012	10 h 55 min
T1307 (Soulik)	Ishigakijima	0700 12 Jul – 1600 12 Jul 2013	9 h
T1312 (Trami)	Ishigakijima	1800 20 Aug – 0700 21 Aug 2013	13 h
T1318 (Man-yi)	Murotomisaki	1300 15 Sep – 1900 15 Sep 2013	6 h
T1323 (Fitow)	Ishigakijima	1300 05 Oct – 0200 06 Oct 2013	13 h
T1324A (Danas)	Okinawa	0200 07 Oct – 1000 07 Oct 2013	8 h
T1324B (Danas)	Naze	0500 07 Oct – 1200 07 Oct 2013	7 h
T1408A (Neoguri)	Ishigakijima	1900 07 Jul – 0110 08 Jul 2014	6 h 10 min
T1408B (Neoguri)	Okinawa	0100 08 Jul – 0410 08 Jul 2014	3 h 10 min
T1411A (Halong)	Naze	0200 08 Aug – 1300 08 Aug 2014	11 h
T1411B (Halong)	Tanegashima	1500 08 Aug – 0500 09 Aug 2014	14 h
T1411C (Halong)	Murotomisaki	1000 09 Aug – 2345 09 Aug 2014	13 h 45 min
T1418A (Phanfone)	Naze	1700 04 Oct – 0400 05 Oct 2014	11 h
T1418B (Phanfone)	Tanegashima	0300 05 Oct – 1100 05 Oct 2014	8 h
T1418C (Phanfone)	Murotomisaki	1330 05 Oct – 1930 05 Oct 2014	6 h
T1419 (Vongfong)	Okinawa	0300 11 Oct – 1200 11 Oct 2014	9 h

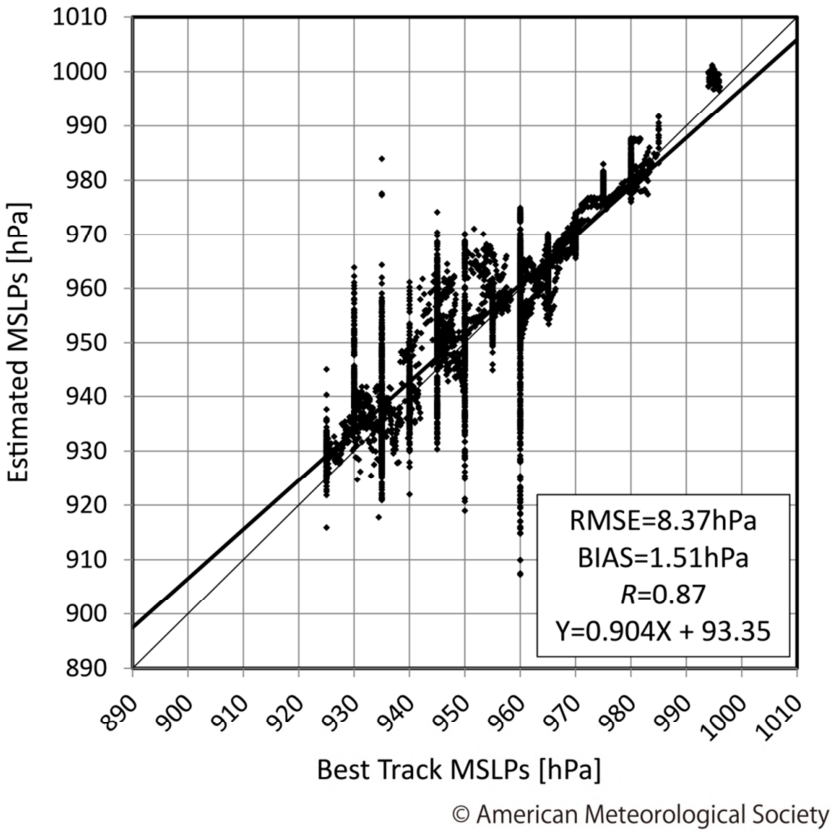

Fig. 2: Comparison of estimated and best-track MSLPs. The corresponding RMSE, bias and correlation coefficient, *R*, are also shown (adapted from SSY).

Table 4. Summary of estimation accuracy in conventional methods

Method	RMSE (hPa)
Dvorak (Koba 1990)	7 – 19
Dvorak (Martin and Gray 1993)	9
Dvorak (Velden et al. 2007)	11.7
AMSU (Oyama 2014)	10.1
AMSU with CIMSS (Velden et al. 2007)	7.5
AMSU with CIRA (Velden et al. 2007)	10.3

b. Accuracy by condition

The accuracy of DR estimates depends on a number of conditions (Fig. 3). The first is the distance between the radar location and the TC center. RMSEs were generally smaller when the distance was shorter, and estimates exhibited a positive bias when the distance was large. This bias may result from the application of the CAPPI method (limitation VII in Subsection 2.2 (b)). The second condition is the distance between the TC center and the weather station whose sea level pressure is used as an anchor for pressure measurement. Large RMSEs with large distances may be attributed to the effect of TC asymmetricity (limitation X in Subsection 2.2 (c)). The general trend of the second condition was the same as that of the first. One possible reason for this is the fact that best-track analysis involves the use of the same weather station observations, and weather stations are located near radar locations. The third condition is the RMW. For TCs with an RMW of 20 – 70 km, estimated central pressure values had an RMSE of 5.55 hPa and showed a bias of 0.69 hPa. In contrast, for TCs with an RMW of 75 – 120 km, the estimates had a large positive bias of 5.23 hPa. For TCs with an RMW below 20 km, estimated MSLPs in T1007 extremely degraded their accuracy. The fourth condition involves radar coverage and the fifth GBVTD retrieval accuracy. As expected, estimated MSLPs tended to be more consistent with best-track MSLPs when radar coverage was denser and wind retrieval accuracy was higher.

SSY examined the relationship between the observational SLP gradient in cases where there were multiple SLP observations around a TC and the corresponding retrieved SLP gradient. The results shown in Fig. 4 indicate that the retrieved SLP gradient was on average 0.55 hPa steeper than the observational SLP gradient over a 44.3 km interval. This result is apparently inconsistent with the general trend of the positive MSLP biases described above. However, given that most of the weather stations were outside the RMW, these findings suggest that the SLP gradient retrieved from outside the RMW is steeper than the actual gradient, and that the SLP gradient inside the RMW, where some values of $\bar{V}_t$ were interpolated using a spline function (limitation XI in Subsection 2.2 (c)), is shallower than the gradient inferred from the best track. This characteristic was also seen in the preliminary experiment described in Subsection 3.1 (not shown).

The reliability of estimated MSLPs should be evaluated in consideration of these specific conditions. The author plans to develop a new index that represents the degree of confidence of estimated MSLPs based on a combination of the conditions in the near future.

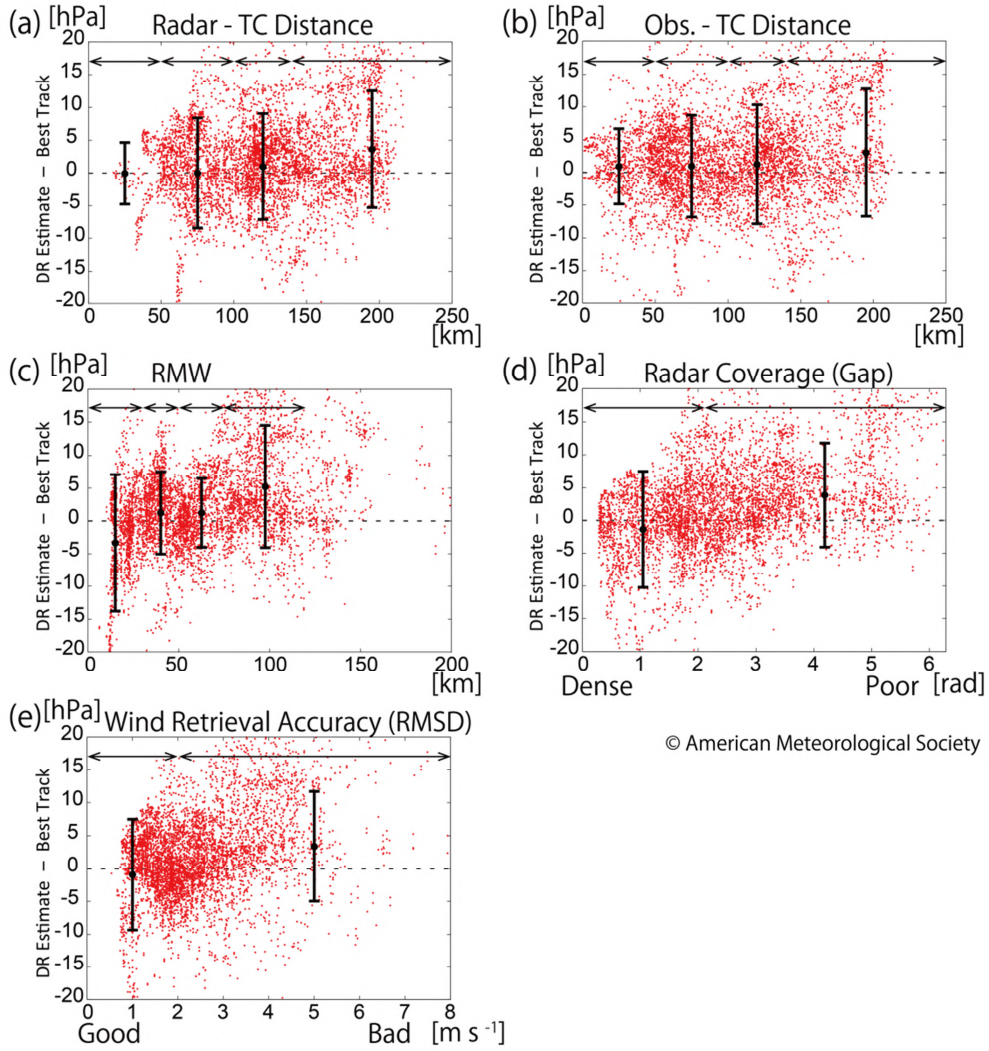

Fig. 3: Comparisons of differences between the estimated MSLPs and the best-track MSLPs (y-axis) with (a) the distance between the radar location and the TC center, (b) the distance between the weather station and the TC center, (c) the RMW at 2-km altitude, (d) radar coverage, and (e) the GBVTD wind retrieval accuracy (x-axis). The RMWs were determined from all retrieved $\bar{V}_t$ after the first step in Fig. 1. The radar coverage is defined as the radial average of the maximum azimuthal gap (rad) at each radius on the GBVTD-specified coordinate system. The wind retrieval accuracy is defined as the overall average of the root mean square difference (RMSD) between the V_D resampled from the GBVTD-retrieved winds and the observed V_D, as per the RMSE shown in Fig. 3 of Zhao et al. (2012). The error bars show the bias and the RMSE within the range indicated by the double-headed arrows (adapted from SSY).

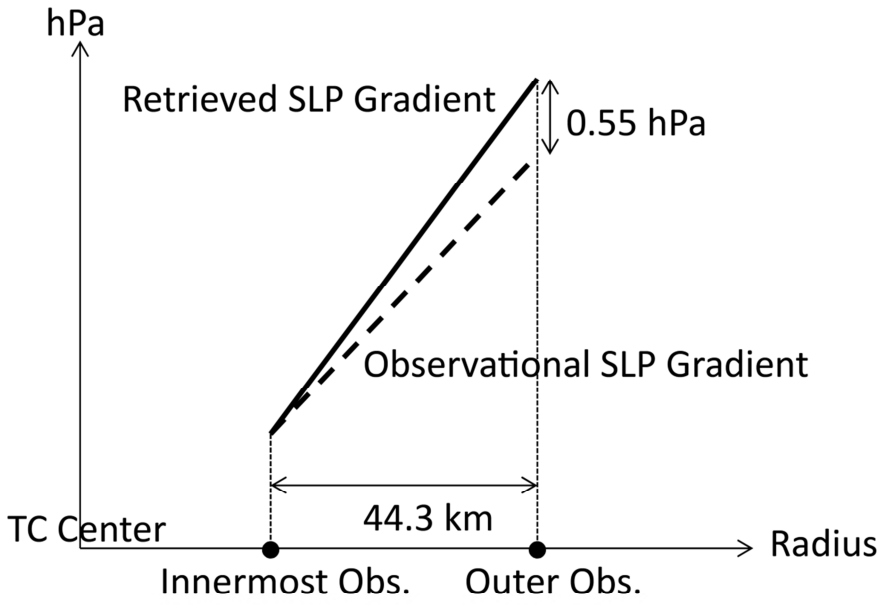

Fig. 4: Retrieved and observed SLP gradients. The values were calculated when data from multiple SLP observations around the TCs were available. To obtain as many SLP gradients in the inner region of TCs as possible, only SLP gradients relative to the innermost observation point were calculated when three or more SLP observations were available (adapted from SSY).

Table 5: Accuracy in the 28 cases examined. The RMW associated with the primary eyewall (P-RMW) was determined from the GBVTD-retrieved $\bar{V}_t$. The P-RMW and central pressure values were averaged over the estimation periods shown in Table 3.

Typhoon	N	Central pressure (hPa)			RMSE (hPa)	BIAS (hPa)	P-RMW (km)
		Estimated	Best track	Dvorak			
T0607 (Maria)	79	998.84	994.96	-	4.08	3.88	27.66
T0709 (Fitow)	226	974.76	974.55	974.44	2.21	0.22	49.12
T0813 (Sinlaku)	106	980.72	981.12	981.92	2.17	-0.41	18.83
T0911 (Krovanh)	137	984.42	980.16	981.00	4.85	4.25	26.95
T1007 (Kompasu)	257	942.93	960.00	947.00	21.60	-17.07	13.13
T1011 (Fanapi)	284	938.03	934.29	947.00	7.23	3.74	36.95
T1109 (Muifa)	243	951.95	945.32	956.00	6.94	6.64	71.68
T1115 (Roke)	49	951.05	949.12	926.86	3.77	1.94	23.19
T1204 (Guchol)	90	936.61	950.00	957.81	14.71	-13.39	38.24
T1210 (Damrey)	165	979.50	975.00	982.17	4.70	4.50	41.23
T1215 (Bolaven)	314	931.66	929.12	948.46	3.88	2.54	14.07
T1216 (Sanba)	258	936.06	933.35	946.01	5.40	2.71	33.12
T1217 (Jelawat)	148	949.92	931.89	947.08	18.87	18.03	85.80
T1307 (Soulik)	203	948.19	948.02	965.00	3.79	0.17	30.89
T1312 (Trami)	299	964.87	965.58	973.00	2.30	-0.70	40.64
T1318 (Man-yi)	140	968.34	960.00	975.75	8.81	8.34	45.10
T1323 (Fitow)	325	963.32	961.33	968.13	2.84	2.00	73.78
T1324 (Danas, T1324A)	336	931.47	935.00	926.00	5.26	-3.53	21.63
T1324 (Danas, T1324B)	166	938.35	935.00	926.00	9.53	3.35	21.01
T1408 (Neoguri, T1408A)	141	940.33	940.00	947.00	3.27	0.33	39.99
T1408 (Neoguri, T1408B)	78	939.70	940.37	947.00	3.12	-0.67	35.21
T1411 (Halong, T1411A)	93	962.88	950.97	959.48	13.00	11.91	91.55
T1411 (Halong, T1411B)	260	956.29	955.32	972.63	3.00	0.97	47.22
T1411 (Halong, T1411C)	574	958.83	961.51	974.21	4.02	-2.68	53.20
T1418 (Phanfone, T1418A)	189	957.21	943.18	953.68	14.99	14.03	92.22
T1418 (Phanfone, T1418B)	167	957.11	945.50	956.00	11.88	11.61	85.55
T1418 (Phanfone, T1418C)	130	958.11	952.91	956.33	6.13	5.21	61.48
T1419 (Vongfong)	117	939.35	945.00	955.29	7.25	-5.65	33.80

4. Case studies

This section outlines four characteristics of DR estimates along with related examples. These are 1) outstanding estimates, 2) large negative differences from the best track, 3) consistent positive differences, and 4) erratic fluctuations in the time evolution of the estimated MSLPs. The causes of these characteristics are discussed in SSY. The Dvorak MSLPs shown in this section were obtained by converting current intensity (CI) numbers archived by the RSMC Tokyo into MSLPs with reference to the conversion table of Koba et al. (1990). Real-time MSLPs were TC intensities provided by the RSMC Tokyo in real time.

Outstanding estimates were defined as those whose average had an RMSE of less than 5 hPa and a bias of less than ±5 hPa. Verification by SSY showed that 50% of estimates (14 of 28; Table 5) met this criterion with the DR method as opposed to only 15% (4 of 27; not shown) with the Dvorak method. Thus, the DR method provided almost the same MSLPs as the best track in about half of all cases in real time. As an example of outstanding estimations, Fig. 5 (a) shows data relating to T1515 as it passed within the range of the Ishigakijima radar (this typhoon was not included in the statistical verification performed by SSY). The RMSE and bias of T1515 were 3.33 and 0.74 hPa, respectively. Goni intensified rapidly after an eyewall replacement, and the MSLPs of the best track were below those of Dvorak estimates. The DR method enabled the capture of the rapid intensity change and deeper MSLPs than those of Dvorak estimates. In addition, GBVTD retrievals highlighted T1515's rapid wind structure change (Figs. 5 (b) – (d)). These results suggest that the DR method is useful not only for MSLP analysis in real time but also for monitoring of structural changes associated with rapid intensity changes.

Second, large negative differences between the DR method and best-track MSLPs were seen in some TCs that were located more than 100 km from the weather station whose central pressure is used as an anchor for pressure measurement and that had a relatively small inner eye (< 30 km). Specifically, T1007, T1204, T1419 and T1509 (T1509 was not included in the statistical verification by SSY) exhibited this characteristic. SSY discussed the possibility that the best track underestimated their MSLPs. Figure 6 shows a time evolution of estimated MSLPs in T1509. The maximum wind increased during the first half of the estimation period, while the RMW decreased slightly and the estimated MSLP deepened. In contrast, the MSLPs of the best track were on average 10 hPa greater than those of the DR method.

Third, in contrast to the second consideration, consistent positive differences were seen in T1109, T1217, T1318, T1418A and T1418B. Other than for T1318, the RMW

associated with the primary eyewall derived from the GBVTD-retrieved $\bar{V}_t$ field was more than 70 km. This is consistent with the trend of the third condition described in Subsection 3.2 (b). Additionally, DR MSLPs were more closely correlated with Dvorak MSLPs than with best-track MSLPs in this group (Table 5). Figure 7 shows time evolutions of estimated MSLPs indicating consistent positive biases in both T1418A and T1418B. SSY proposed that when the RMW is large, the effect of the difference between SLP structures inside the RMW assumed in best-track analysis and deduced from the DR method on MSLP estimates may be large, and thus application of the DR method may improve the quality of best-track analysis.

Fourth, erratic fluctuations in MSLP estimates were seen in most cases. Such fluctuations can be classified as those with a period of a few hours and those with fine erratic variations of around 5 hPa at 5-min intervals. An example of the former is seen with T1521 (Fig. 8 (a); T1521 was not included in the statistical verification performed by SSY). This TC had an elliptic eyewall (Fig. 8 (b)), which caused wavenumber-2 radial wind dominance that could have caused bias in estimated MSLPs with a period of a few hours (limitation III in Subsection 2.2 (a)). In addition, T1521 exhibited relatively large fluctuations at the end of the period due to noise contamination caused by dealiasing correction failure (limitation VIII in Subsection 2.2 (b)). The estimated MSLPs of T1515 exhibited typical fine erratic fluctuations (Fig. 5 (a)) probably attributable to center location errors (limitation I in Subsection 2.2 (a)). Limitation IV (Subsection 2.2 (a)) may also have caused fluctuations with an amplitude of 5 – 15 hPa in T1324 (Fig. 9 (a)), while the estimated MSLPs of T1411 fluctuated wildly between the two extremes due to limitation IX as described in Subsection 2.2 (b) (Fig. 9 (b)).

Given these estimation result characteristics, the use of a running mean of DR MSLPs covering a few hours is advisable (as shown by the black lines in Figs. 5 – 9). Additionally, by paying attention to the characteristics of each group, analysts should be able to utilize these MSLPs with higher accuracy and reliability than is suggested by the overall accuracy described in Subsection 3.2 (a).

In summary, the DR method generally provides estimates of TC intensity accurately enough to be used operationally if applied appropriately with full understanding of its technical utility and limitations. The use of DR estimates would represent a new paradigm for intensity analysis in the western North Pacific, where aircraft observations are not available.

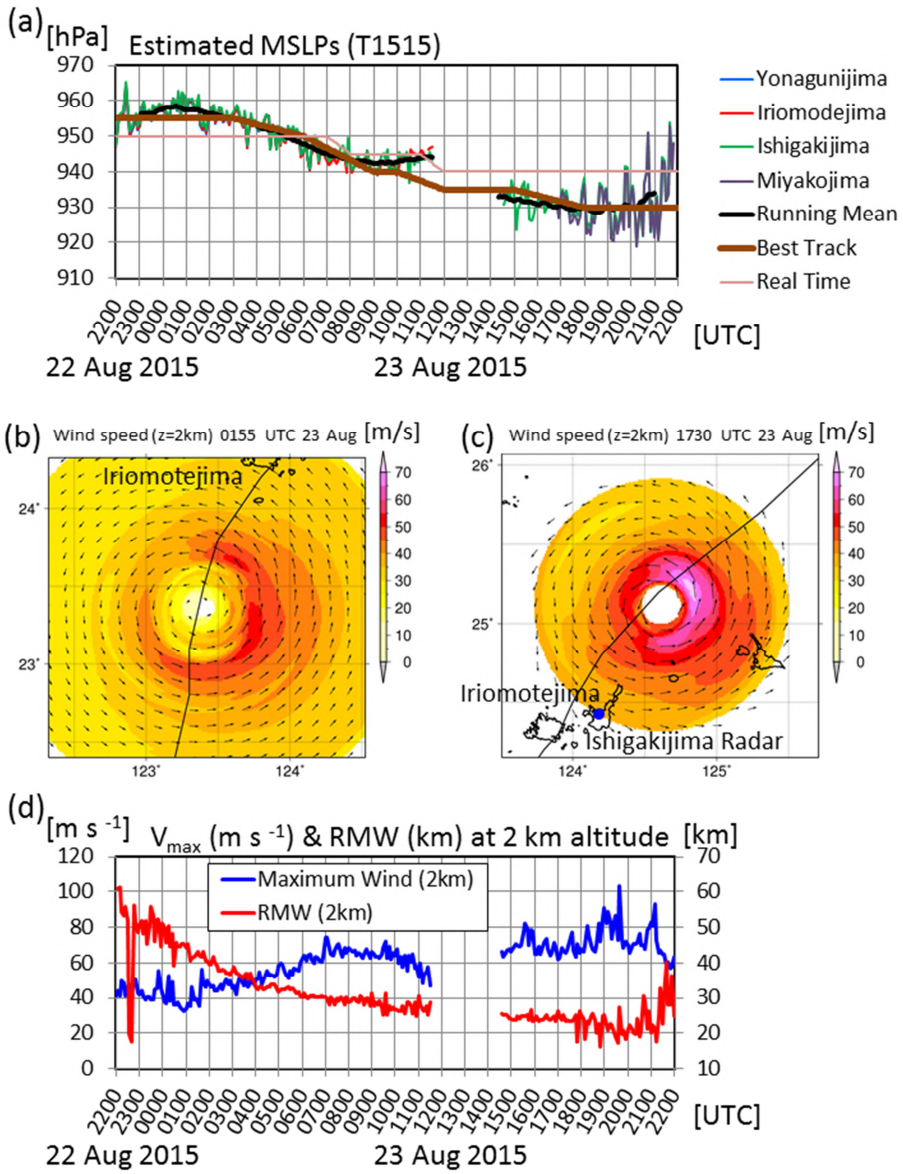

Fig. 5: (a) Time evolutions of the DR MSLPs (blue, red, green and purple lines), their running means (2 hours; black line), best-track MSLPs (brown line) and real-time MSLPs (pink line) for T1515 (Typhoon Goni). The blue, red, green and purple lines indicate MSLPs derived from SLPs at Yonaguni, Iriomotejima, Ishigakijima and Miyakojima, respectively. (b) The GBVTD-retrieved wind speed at 2-km altitude based on V_D observed by the Ishigakijima radar (blue dot) at 0155 UTC on 23 August 2015. (c) Same as (b), except for 1730 UTC on 23 August 2015. (d) Time evolutions of the maximum wind and RMW at 2-km altitude for T1515.

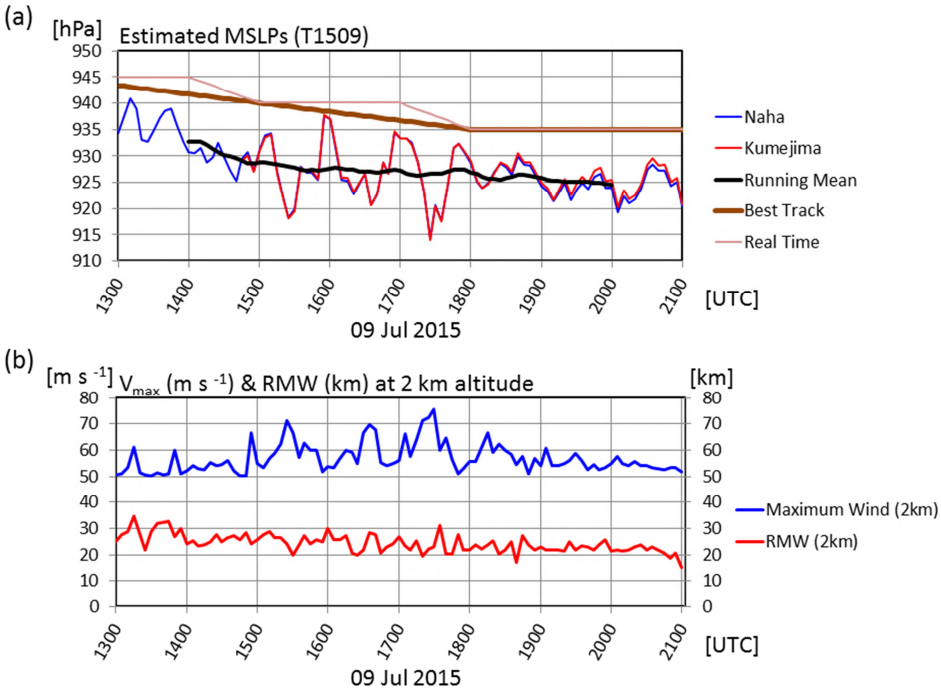

Fig. 6: (a) Time evolutions of the DR MSLPs (blue and red lines) and their running mean (2 hours; black line), best-track MSLPs (brown line) and real-time MSLPs (pink line) for T1509 (Typhoon Chan-hom). The blue and red lines indicate MSLPs derived from SLPs at Naha and Kumejima, respectively. (b) Time evolutions of the maximum wind and RMW at 2-km altitude for T1509.

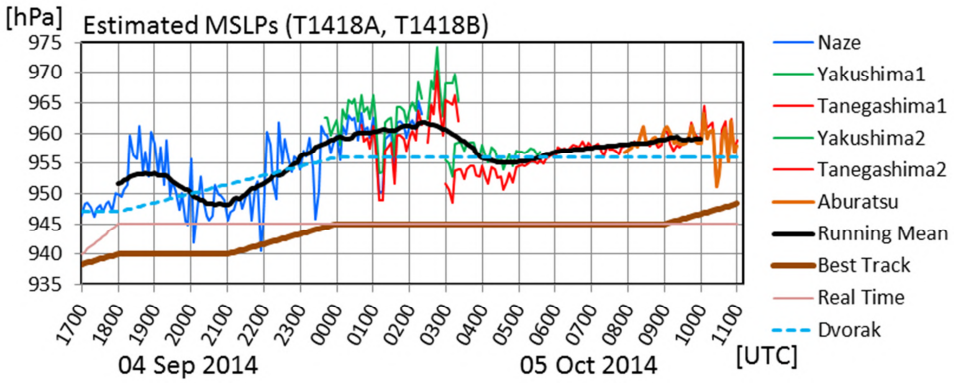

Fig. 7: Time evolutions of the DR MSLPs (blue, green, red and orange lines), their running mean (2 hours; black line), best-track MSLPs (brown line), real-time MSLPs (pink line) and Dvorak MSLPs (light-blue dashed line) for T1418A and T1418B (Typhoon Phanfone). The blue, green, red and orange lines indicate MSLPs derived from SLPs at Naze, Yakushima, Tanegashima and Aburatsu, respectively.

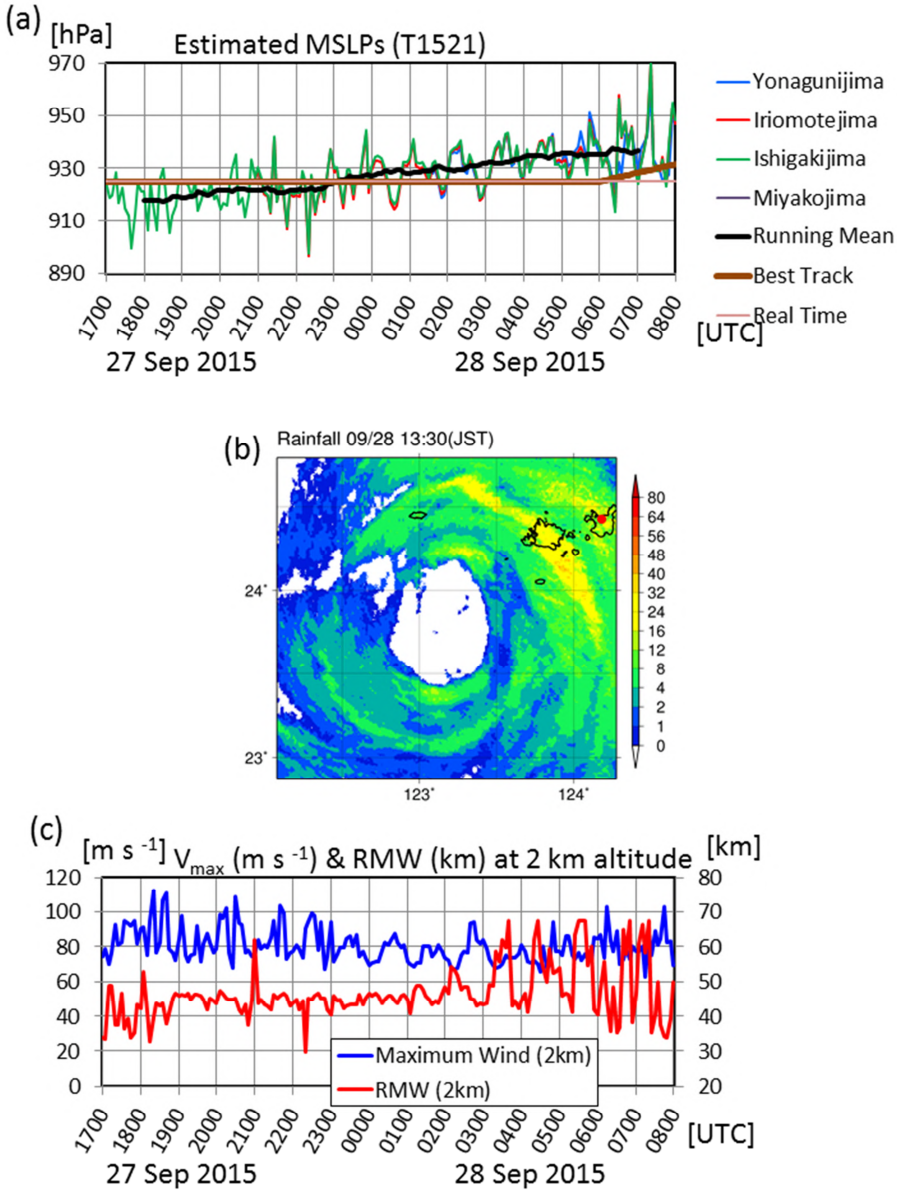

Fig. 8: (a) Time evolutions of the DR MSLPs (blue, red, green and purple lines), their running mean (2 hours; black line), best-track MSLPs (brown line) and real-time MSLPs (pink line) for T1521 (Typhoon Dujuan). The blue, red, green and purple lines indicate MSLPs derived from SLPs at Yonaguni, Iriomotejima, Ishigakijima and Miyakojima, respectively. (b) Radar composite imagery for 0430 UTC on 28 September 2015. (c) Time evolutions of the maximum wind and RMW at 2-km altitude for T1521.

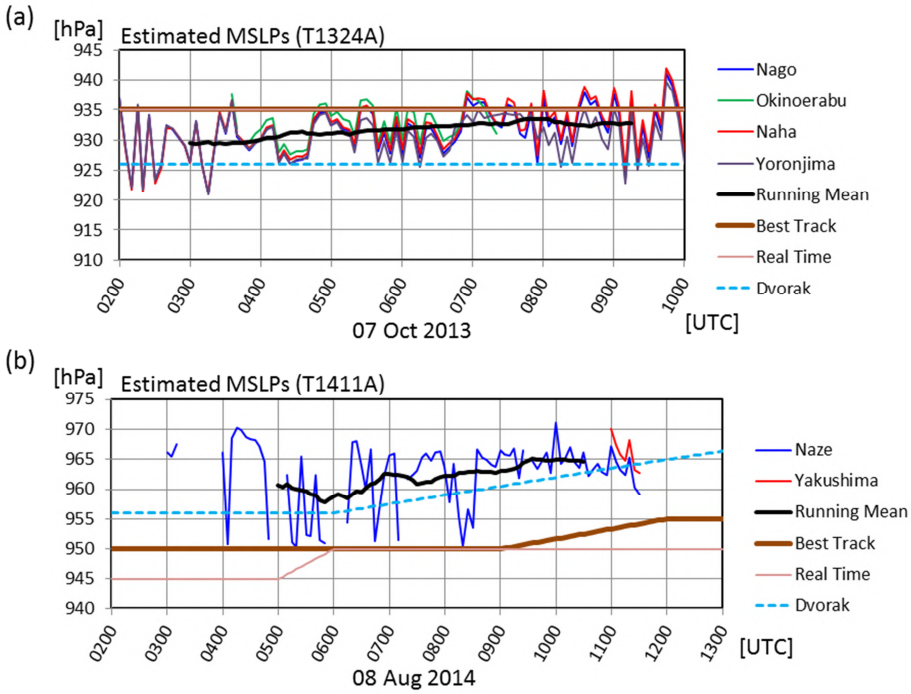

Fig. 9: (a) Time evolutions of the DR MSLPs (blue, green, red and purple lines), their running mean (2 hours; black line), best-track MSLPs (brown line), real-time MSLPs (pink line) and Dvorak MSLPs (light-blue dashed line) for T1324A (Typhoon Danas). The blue, green, red and purple lines indicate MSLPs derived from SLPs at Nago, Okinawa, Naha and Yoronjima, respectively. (b) Time evolutions of the DR MSLPs (blue and red lines), their running mean (2 hours; black line), best-track MSLPs (brown line), real-time MSLPs (pink line) and Dvorak MSLPs (light-blue dashed line) for T1411A (Typhoon Halong). The blue and red lines indicate MSLPs derived from SLPs at Naze and Yakushima, respectively.

5. Summary

The MRI/JMA developed a new system for estimating the intensity (central pressure) of TCs at 5-min intervals using single ground-based Doppler radar observations. The method involves the use of the ground-based velocity track display (GBVTD) technique, in which tangential winds are retrieved, and the gradient wind balance. In terms of the accuracy of this method, the root mean square error (RMSE) and bias are 8.37 and 1.51 hPa, respectively, relative to the best track data of the RSMC Tokyo. This level of accuracy is comparable to or better than the accuracies of conventional methods such as Dvorak and satellite microwave-derived estimates. With the DR method, 50% of estimates met the criterion of an RMSE less than 5 hPa and the bias was within ±5

hPa, while only 15% of estimates met the same criterion with the Dvorak method. In addition, for TCs with an RMW of 20 – 70 km, the estimated central pressures had an RMSE of 5.55 hPa. Estimation accuracy was generally higher with shorter distances between the TC center and the radar location and between the TC center and the weather station whose sea level pressure was used as an anchor for pressure measurement, as well as when wind retrieval accuracy was higher and radar coverage was denser. These facts suggest that the method enables TC monitoring at 5-min intervals from a few hours before landfall in populated areas and helps to clarify intensity changes in real time.

Time evolutions of MSLPs estimated using the DR method showed four notable characteristics that should be considered in operational use. First, there are erratic fluctuations of between 5 and 15 hPa in estimates made at 5-min intervals. Second, TCs with polygonal eyewall structure can exhibit artificial MSLP fluctuations with periods of a few hours. These two points are probably attributable to technical limitations, and DR estimates should therefore be time-filtered or averaged for accuracy. Third, TCs with RMWs exceeding 70 km tend to have a consistent positive bias relative to the best track. Fourth, in some cases, when the distance between the TC center and the weather station is more than 100 km and when the TC has a distinct, relatively small eye, estimates can have large negative biases relative to the best track. These last two points, however, do not necessarily mean that DR estimates have large errors; rather, they suggest the possibility that the DR method can capture some TC intensity changes that the conventional methods fail to capture. Thus, the operational use of the approach is expected to contribute to more accurate intensity analysis for TCs approaching Japan.

Based on these characteristics, the use of DR estimates can be considered valuable for reducing the uncertainty of TC intensity analysis in the western North Pacific, where aircraft observations are unavailable, if used appropriately with full understanding of its technical utility and limitations.

References

Aberson, S. D., M. T. Montgomery, M. Bell, and M. Black, 2006: Hurricane Isabel (2003): New insights into the physics of intense storms. Part II: Extreme localized wind. *Bull. Amer. Meteor. Soc.*, **87,** 1349–1354, doi:10.1175/BAMS-87-10-1349.

Bell, M. M., and M. T. Montgomery, 2008: Observed structure, evolution, and potential intensity of category 5 Hurricane Isabel (2003) from 12 to 14 September. *Mon. Wea. Rev.*, **136**, 2023–2046, doi:10.1175/2007MWR1858.1.

Braun, S. A., M. T. Montgomery, and Z. Pu, 2006: High-resolution simulation of

Hurricane Bonnie (1998). Part I: The organization of eyewall vertical motion. *J. Atmos. Sci.*, **63**, 19–42, doi:10.1175/JAS3598.1.

Chen, X., K. Zhao, W.-C. Lee, B. J.-D. Jou, M. Xue, and P. R. Harasti, 2013: The improvement to the environmental wind and tropical cyclone circulation retrievals with Modified GBVTD (MGBVTD) technique. *J. Appl. Meteor. Climatology,* **52**, 2493-2508, doi:10.1175/JAMC-D-13-031.1.

Dvorak, V. F., 1975: Tropical cyclone intensity analysis and forecasting from satellite imagery. Mon. Wea. Rev., **103**, 420 – 430, doi:10.1175/1520-0493(1975)103<0420:TCIAAF>2.0.CO;2.

Dvorak, V. F., 1984: Tropical cyclone intensity analysis using satellite data. NOAA Tech. Rep. **11**, 45 pp.

Franklin, J. L., M. L. Black, and K. Valde, 2003: GPS dropwindsonde wind profiles in hurricanes and their operational implications. *Wea. Forecasting*, **18,** 32–44, doi:10.1175/1520-0434(2003)018<0032:GDWPIH>2.0.CO;2.

Harasti, P. R., W.-C. Lee, and M. Bell, 2007: Real-time implementation of VORTRAC at the National Hurricane Center. Preprints, *33rd Conf. on Radar Meteorology,* Cairns, Australia, Amer. Meteor. Soc., P11A.6. [Available online at https://ams.confex.com/ams/33Radar/webprogram/Paper123747.html]

Harasti, P. R., C. J. McAdie, P. P. Dodge, W.-C. Lee, J. Tuttle, S. T. Murillo, and F. D. Marks, 2004: Real-time implementation of single-Doppler radar analysis methods for tropical cyclones: Algorithm improvements and use with WSR-88D display data. *Wea. Forecasting*, **19**, 219–239, doi:10.1175/1520-0434(2004)019<0219:RIOSRA>2.0.CO;2.

Hoshino, S. and T. Nakazawa, 2007: Estimation of tropical cyclone's intensity using TRMM/TMI brightness temperature data. J. Meteor. Soc. Japan, **85**, 437 – 454, doi:10.2151/jmsj.85.437.

Kepert, J. D., 2006a: Observed boundary layer wind structure and balance in the hurricane core. Part I: Hurricane Georges. *J. Atmos. Sci.*, **63**, 2169–2193, doi:10.1175/JAS3745.1.

Kepert, J. D., 2006b: Observed boundary layer wind structure and balance in the Hurricane core. Part II: Hurricane Mitch. *J. Atmos. Sci.*, **63**, 2194–2211, doi:10.1175/JAS3746.1.

Kishimoto, K., M. Sasaki, and M. Kunitsugu, 2013: Cloud Grid Information Objective Dvorak Analysis (CLOUD) at the RSMC Tokyo - Typhoon Center. RSMC Tokyo - Typhoon Center Tech. Rev., No. **15**.

Koba, H., T. Hagiwara, S. Osano, and S. Akashi, 1990: Relationship between the

CI-number and central pressure and maximum wind speed in typhoons (in Japanese). *J. Meteor. Res.,* **42,** 59–67.

Kossin, J. P., and W. H. Schubert, 2004: Mesovortices in Hurricane Isabel. *Bull. Amer. Meteor. Soc.*, **85**, 151–153, doi:10.1175/BAMS-85-2-151.

Lee, W.-C., and F. D. Marks Jr., 2000: Tropical cyclone kinematic structure retrieved from single-Doppler radar observations. Part II: The GBVTD-simplex center finding algorithm. *Mon. Wea. Rev.*, **128**, 1925–1936, doi:10.1175/1520-0493(2000)128<1925:TCKSRF>2.0.CO;2.

Lee, W.-C., B. J.-D. Jou, P.-L. Chang, and S.-M. Deng, 1999: Tropical cyclone kinematic structure retrieved from single-Doppler radar observations. Part I: Interpretation of Doppler velocity patterns and the GBVTD technique. *Mon. Wea. Rev.*, **127**, 2419–2439, doi:10.1175/1520-0493(1999)127<2419:TCKSRF>2.0.CO;2.

Marks, F. D., P. G. Black, M. T. Montgomery, and R. W. Burpee, 2008: Structure of the eye and eyewall of Hurricane Hugo (1989). *Mon. Wea. Rev.*, **136**, 1237–1259, doi:10.1175/2007MWR2073.1.

Martin, J. D., and W. M. Gray, 1993: Tropical cyclone observation and forecasting with and without aircraft reconnaissance. *Wea. Forecasting*, **8**, 519–532, doi:10.1175/1520-0434(1993)008<0519:TCOAFW>2.0.CO;2.

Montgomery, M. T., and R. J. Kallenbach, 1997: A theory for vortex Rossby waves and its application to spiral bands and intensity changes in hurricanes. *Quart. J. Roy. Meteor. Soc.*, **123,** 435–465, doi:10.1002/qj.49712353810.

Murillo, S. T., W.-C. Lee, M. M. Bell, F. D. Marks Jr., P. P. Dodge, and G. M. Barnes, 2011: Intercomparison of ground-based velocity track display (GBVTD)-retrieved circulation centers and structures of Hurricane Danny (1997) from two coastal WSR-88Ds. *Mon. Wea. Rev.*, **139**, 153–174, doi:10.1175/2010MWR3036.1.

Ogura, Y., 1964: Frictionally controlled, thermally driven circulations in a circular vortex with application to tropical cyclones. *J. Atmos. Sci.*, **21**, 610–621, doi:10.1175/1520-0469(1964)021<0610:FCTDCI>2.0.CO;2.

Oyama, R., 2014: Estimation of tropical cyclone central pressure from warm core intensity observed by the Advanced Microwave Sounding Unit-A (AMSU-A), *Pap. Meteor. Geophys.*, **65**, 35-56, doi:10.2467/mripapers.65.35.

Sakuragi, T., S. Hoshino and N. Kitabatake, 2014: Development and verification of a tropical cyclone intensity estimation method reflecting the variety of TRMM/TMI brightness temperature distribution. RSMC Tokyo - Typhoon Center Tech. Rev., No. **16**.

Shimada, U., M. Sawada, and H. Yamada, 2016: Evaluation of the Accuracy and Utility

of Tropical Cyclone Intensity Estimation Using Single Ground-Based Doppler Radar Observations. Mon. Wea. Rev., 144, 1823-1840, doi:10.1175/MWR-D-15-0254.1.

Velden, C., D. Herndon, J. Kossin, J. Hawkins, and M. DeMaria, 2007: Consensus estimates of tropical cyclone (TC) intensity using integrated multispectral (IR and MW) satellite observations. *Joint 2007 EUMETSAT Meteorological Satellite & 15th AMS Satellite Meteorology and Oceanography conference*, Amsterdam, The Netherlands. [Available online at http://www.ssec.wisc.edu/meetings/jointsatmet2007/pdf/velden_satcon.pdf]

Wang, Y., 2002: Vortex Rossby waves in a numerically simulated tropical cyclone. Part I: Overall structure, potential vorticity, and kinetic energy budgets. *J. Atmos. Sci.*, **59**, 1213–1238, doi:10.1175/1520-0469(2002)059<1213:VRWIAN>2.0.CO;2.

Willoughby, H. E., 1990: Gradient balance in tropical cyclones. *J. Atmos. Sci.*, **47**, 265–274, doi:10.1175/1520-0469(1990)047<0265:GBITC>2.0.CO;2.

Yamauchi, H., O. Suzuki, and K. Akaeda, 2006: A hybrid multi-PRI method to Dealias Doppler velocities. *SOLA*, **2**, 92-95, doi:10.2151/sola.2006-024.

Zhao, K., M. Xue, and W.-C. Lee, 2012: Assimilation of GBVTD-retrieved winds from single-Doppler radar for short-term forecasting of super typhoon Saomai (0608) at landfall. *Quart. J. Roy. Meteor. Soc.,* **138**, 1055–1071, doi:10.1002/qj.975.